



# New fluorescent auxin derivatives: anti-auxin activity and accumulation patterns in *Arabidopsis thaliana*

Kristýna Bielešová<sup>1</sup> · Pavel Hladík<sup>2</sup> · Martin Kubala<sup>3</sup> · Richard Napier<sup>4</sup> · Federica Brunoni<sup>2</sup> · Zuzana Gelová<sup>5</sup> · Lukáš Fiedler<sup>5</sup> · Ivan Kulich<sup>5</sup> · Miroslav Strnad<sup>2</sup> · Karel Doležal<sup>1,2</sup> · Ondřej Novák<sup>2</sup> · Jiří Friml<sup>5</sup> · Asta Žukauskaitė<sup>1</sup>

Received: 18 July 2023 / Accepted: 14 September 2023  
© The Author(s) 2023

## Abstract

Auxin belongs among major phytohormones and governs multiple aspects of plant growth and development. The establishment of auxin concentration gradients, determines, among other processes, plant organ positioning and growth responses to environmental stimuli.

Herein we report the synthesis of new NBD- or DNS-labelled IAA derivatives and the elucidation of their biological activity, fluorescence properties and subcellular accumulation patterns *in planta*. These novel compounds did not show auxin-like activity, but instead antagonized physiological auxin effects. The DNS-labelled derivatives **FL5** and **FL6** showed strong anti-auxin activity in roots and hypocotyls, which also occurred at the level of gene transcription as confirmed by quantitative PCR analysis. The auxin antagonism of our derivatives was further demonstrated *in vitro* using an SPR-based binding assay. The NBD-labelled compound **FL4** with the best fluorescence properties proved to be unsuitable to study auxin accumulation patterns *in planta*. On the other hand, the strongest anti-auxin activity possessing compounds **FL5** and **FL6** could be useful to study binding mechanisms to auxin receptors and for manipulations of auxin-regulated processes.

**Keywords** Anti-auxin · *Arabidopsis* · Fluorescent label · Biological activity · Indole-3-acetic acid (IAA), Transport inhibitor response 1 (TIR1)

---

Communicated by J. Celenza.

✉ Asta Žukauskaitė  
asta.zukauskaite@upol.cz

- <sup>1</sup> Department of Chemical Biology, Faculty of Science, Palacký University, Šlechtitelů 27, Olomouc CZ-78371, Czech Republic
- <sup>2</sup> Laboratory of Growth Regulators, Faculty of Science, Palacký University & Institute of Experimental Botany, The Czech Academy of Sciences, Šlechtitelů 27, Olomouc CZ-78371, Czech Republic
- <sup>3</sup> Department of Experimental Physics, Faculty of Science, Palacký University, 17. listopadu 12, Olomouc CZ-77146, Czech Republic
- <sup>4</sup> School of Life Sciences, University of Warwick, Coventry CV47AL, UK
- <sup>5</sup> Institute of Science and Technology Austria, Am Campus 1, Klosterneuburg 3400, Austria

## Introduction

Phytohormones regulate plant growth, development, and responses to both internal and external stimuli *via* a complex network of signalling pathways (Hemelíková et al. 2021; Friml 2022). The structures and main roles of classical phytohormones have been known for decades. Combining this knowledge with synthetic chemistry has allowed the creation of a wide array of synthetic phytohormone analogues including agonists, antagonists, or caged and labelled derivatives. These compounds can be used to manipulate plant growth or serve as powerful tools for obtaining new insights into the modes of action of phytohormones (Rigal et al. 2014; Jiang and Asami 2018; Hemelíková et al. 2021).

Auxin is a key phytohormone, which controls cell division, elongation and differentiation, tropic responses, etc. (Woodward and Bartel 2005). The canonical/transcriptional auxin signalling pathway relies on the action of three main protein families: (i) Transport Inhibitor Response 1/Auxin Signalling F-box proteins (TIR1/AFBs) (Dharmasiri et

al. 2005b; Mockaitis and Estelle 2008; Caumon and Vernoux 2023), (ii) the Aux/IAA transcriptional co-repressors (Remington et al. 2004; Overvoorde et al. 2005), and (iii) Auxin Response Factors (ARFs) (Okushima et al. 2005; Guilfoyle and Hagen 2007). Under low cellular levels of auxin, Aux/IAAs repress the ARF-dependent transcription of auxin-responsive genes. On the other hand, under higher concentrations, auxins enable the interaction of domain II of Aux/IAA transcriptional co-repressors with TIR1/AFB F-box proteins. This leads to Aux/IAA ubiquitination by the Skp1-Cullin-F-box (SCF)<sup>TIR1/AFB</sup> E3 ligase and to Aux/IAA targeting for degradation. Degradation of Aux/IAAs derepresses ARF proteins, which allows them to modulate the transcription of auxin-responsive genes (Santner et al. 2009). Recently, auxin perception was shown to stimulate the production of a second messenger known from animals, cyclic adenosine monophosphate (cAMP), and TIR1/AFB receptors have been demonstrated to possess adenylylate cyclase activity (Qi et al. 2022). Besides TIR1/AFBs, Auxin-binding Protein 1 (ABP1) and its plasma membrane-localized partner, Transmembrane Kinase 1 (TMK1), have been reported to be required for an auxin-induced ultrafast global phospho-response, activation of plasma-membrane H<sup>+</sup>-ATPases and acceleration of cytoplasmic streaming (Friml et al. 2022).

Besides indole-3-acetic acid (IAA) and other naturally occurring auxins (Sauer et al. 2013), numerous synthetic compounds with auxin-like activities have been identified (Jiang and Asami 2018). For instance, dichlorophenoxyacetic acid (2,4-D), 3,6-dichloro-2-methoxybenzoic acid (dicamba), etc., inhibit plant growth, and induce senescence and tissue decay in sensitive dicots, making synthetic auxins applicable as plant growth regulators and herbicides (Grossmann 2010; Todd et al. 2020). On the other hand, 4-(2,4-dimethylphenyl)-2-(1*H*-indol-3-yl)-4-oxobutanoic acid (auxinole), 2-(1*H*-indol-3-yl)-4-oxo-4-phenylbutanoic acid (PEO-IAA), or 4-([1,1'-biphenyl]-4-yl)-2-(1*H*-indol-3-yl)-4-oxobutanoic acid (BP-IAA) and its methoxy derivatives possess anti-auxin activity (Hayashi et al. 2012; Žukauskaitė et al. 2023). These derivatives found use in both agriculture and basic plant science to study various biological phenomena (Rigal et al. 2014; Jiang and Asami 2018). Auxinole has been demonstrated to block auxin-induced Ca<sup>2+</sup> signalling in root cells (Dindas et al. 2018), to decrease auxin-mediated increase in the density of actin filaments in root epidermal cells (Scheuring et al. 2016) and to accelerate petal abscission (Liang et al. 2020). PEO-IAA suppresses root gravitropism and enhances root phototropism (Kimura et al. 2018), and causes chromatin loosening upon application to proliferating plant cells (Hasegawa et al. 2018). The agricultural potential of anti-auxins has also been demonstrated; PEO-IAA was reported to improve

grain yield in rice (Tamaki et al. 2015), while both PEO-IAA and BP-IAA derivatives improve in vitro propagation of *Cannabis sativa* L. (Smýkalová et al. 2019; Šenkyřík et al. 2023; Žukauskaitė et al. 2023).

Auxin-sensitive reporter lines such as DR5::GUS, DR5::GFP or DII::VENUS are widely used to study dynamic auxin distribution in plant tissues (Pařízková et al. 2017). However, such auxin-sensitive reporter lines are limited to several model species and, even then, only semi-quantitative in vivo imaging of local substrate concentrations can be achieved (Geisler 2018; Balcerowicz et al. 2021). The recently developed genetically encoded AuxSen biosensor is based on auxin binding to a tryptophan repressor (TrpR), which enables quantitative Förster resonance energy transfer (FRET)-based in vivo visualization of auxin (Herud-Sikimić et al. 2021). As an alternative, efforts have been made to develop fluorescently labelled phytohormones (Lace and Prandi 2016). However, even if the selected fluorescent label is relatively small, its attachment might change the biological activity of the phytohormone due to alterations in hydrophobicity/hydrophilicity, solubility, charge, etc. Therefore, when developing fluorescently labelled compounds, it is essential to optimally choose the labelling site, the fluorophore and the type of linker for preservation of biological activity as well as fluorescence properties (Shani et al. 2013; Prandi et al. 2014; Malachowska-Ugarte et al. 2015).

## Materials and methods

### Synthesis of compounds

Detailed synthetic procedures and spectral data of the compounds are described in Supplementary Information.

### Investigation of fluorescence properties

#### Absorption spectra

Absorption spectra of 2 μM solutions of NBD-labelled compound **FL4** and DNS-labelled compounds **FL5**, **FL6** in methanol were recorded on a SP-UV1100 spectrometer (DLAB Scientific) in a quartz cuvette with 1 cm optical path, and a pure solvent was used as a reference. The spectra were measured in the 250–550 nm interval with 1 nm step and 2 nm bandpass. The extinction coefficient  $\epsilon(\lambda)$  was calculated from the formula:

$$\epsilon(\lambda) = \frac{A(\lambda)}{cl}$$

where  $A(\lambda)$  is the estimated absorbance,  $c$  is the sample concentration and  $l$  is the optical path.

### Steady-state fluorescence spectra

Steady-state excitation and emission spectra of 2  $\mu\text{M}$  solutions of compounds **FL4**, **FL5** and **FL6** in methanol were recorded on a Fluorolog-3 fluorometer (Jobin-Yvon, France) in a quartz cuvette with 1 cm optical path (both in excitation and emission). The absorbance of the sample at the excitation wavelength should be below 0.05 in all cases, and therefore the inner-filter effect could be neglected. Emission spectra for NBD-labelled compound **FL4** were recorded with excitation at 480 nm, bandpasses in both the excitation and emission monochromator were set to 3 nm, the spectra were scanned with 1 nm steps and integration time 0.5 s per data point at 22 °C. Emission spectra for DNS-labelled compounds **FL5** and **FL6** were recorded with excitation at 360 nm, bandpasses in both the excitation and emission monochromator were set to 2 nm, the spectra were scanned with 1 nm steps and integration time 0.2 s per data point at 22 °C.

### Quantum yield (QY) estimation

Emission spectra were acquired under conditions described above. For NBD-labelled compound **FL4** and DNS-labelled derivatives **FL5** and **FL6** fluorescence intensity was integrated in the 485–700 nm and 370–700 nm intervals, respectively, and the quantum yield (QY) was calculated from the formula:

$$QY = \frac{\epsilon_S F n^2}{\epsilon F_S n_S^2} QY_S$$

where for NBD-labelled compound **FL4**  $\epsilon$ ,  $F$  and  $n$  refer to the extinction coefficient at 480 nm, integrated fluorescence intensity and refractive index, respectively, the subscript „S“ refers to the standard (1 nM fluorescein in 0.1 M NaOH,  $QY_S = 0.95$ ) (Brannon and Magde 1978), while for DNS-labelled compounds **FL5** and **FL6**  $\epsilon$ ,  $F$  and  $n$  refer to the extinction coefficient at 360 nm, integrated fluorescence intensity and refractive index, respectively, the subscript „S“ refers to the standard (2.5  $\mu\text{M}$  quinine sulphate in 0.05 M  $\text{H}_2\text{SO}_4$ ,  $QY_S = 0.60$ ) (Suzuki et al. 2009).

### Biological activity evaluation

#### Plant growth conditions

Prior to use, all *Arabidopsis thaliana* seeds were sterilized in 70% ethanol with 0.1% Tween-20 solution for 10 min (2×)

and rinsed with 96% ethanol for 10 min. After 2 days of stratification (4 °C in dark), seeds were germinated on sterile  $\frac{1}{2}$  MS medium (2.2 g/L Murashige and Skoog medium, 1% sucrose, 0.5 g/L MES PUFFERAN and 0.7% agar, pH 5.6) in a growth chamber under long-day light conditions (22 °C/20 °C, 16 h light/8 h dark, 100  $\mu\text{mol m}^{-2} \text{s}^{-1}$ ) in a vertical position for indicated time.

#### Effects of synthesized compounds on auxin signalling in DR5::GUS *Arabidopsis thaliana* transgenic plants

Five-day-old seedlings of *Arabidopsis thaliana* seeds expressing DR5::GUS (Ulmasov et al. 1997) in the Col-0 background were incubated in 24-well plates containing 1 mL of  $\frac{1}{2}$  MS liquid medium supplemented with 0.5% DMSO as a blank control, 1  $\mu\text{M}$  IAA as a positive control or derivatives **FL1-6** either on their own at 20  $\mu\text{M}$  concentration or at 5, 10 and 20  $\mu\text{M}$  with 1  $\mu\text{M}$  IAA. The compounds were applied for 5 h. Seedlings were then incubated in 500  $\mu\text{L}$  of GUS staining solution (Na-phosphate buffer, pH 7.0: 4.7 g of  $\text{NaH}_2\text{PO}_4 \cdot \text{H}_2\text{O}$ , 9.6 g of  $\text{Na}_2\text{HPO}_4 \cdot 2 \text{H}_2\text{O}$  was dissolved in 500 mL of distilled water to give 200 mM stock solution. Fifty mL of Na-phosphate buffer were supplemented with 0.08 g  $\text{K}_3[\text{Fe}(\text{CN})_6]$ , 0.12 g  $\text{K}_4[\text{Fe}(\text{CN})_6]$ , 50  $\mu\text{L}$  0.1% Triton and 50 mg of X-Gluc dissolved in 500  $\mu\text{L}$  of DMSO) (Žukauskaitė et al. 2023) at 37 °C in the dark for 30 min. To stop the staining reaction, seedlings were transferred to 500  $\mu\text{L}$  of 70% ethanol and kept overnight. Roots were cleared with HCG-2 solution (120 g chloral hydrate, 90 mL water, 30 mL glycerol) (Ma et al. 2020). GUS expression was evaluated using an inverted light microscope (Olympus IX51) with a transmission light mode under phase contrast. Experimental set up involved 10× objective.

#### Effects of synthesized compounds on root growth and auxin signalling in DR5::LUC *Arabidopsis thaliana* transgenic plants

Five-day-old *Arabidopsis thaliana* seedlings expressing DR5::LUC (Moreno-Risueno et al. 2010) in the Col-0 background (10–15 seedlings per treatment) were transferred to plates containing sterile  $\frac{1}{2}$  MS supplemented with 0.3% DMSO as a blank control, 0.1  $\mu\text{M}$  IAA as positive control or compounds **FL4**, **FL5** and **FL6** at a final concentration of 10  $\mu\text{M}$  with or without 0.1  $\mu\text{M}$  IAA. Immediately, treated plates were placed on a flatbed scanner (Epson, model: V370 Photo). Samples were automatically scanned in the 8-bit grayscale mode and at 800 dpi every 10 min using the Autolt program for 6 h. Afterwards, the shoots were cut off and roots were collected in 2 mL Eppendorf tubes (with 2 iron beads inside) and flash-frozen in liquid nitrogen. Samples were ground with Retsch mill and then 700  $\mu\text{L}$  of

Cell Culture Lysis reagent (CCLR, 5× diluted in water) was added. Then the samples were mixed, centrifuged and left for 2 min on ice. Subsequently, 100 µL of lysate was transferred to a microtiter plate and assayed with a luminometer (BioTek Synergy H1 Plate Reader) using Luciferase Assay Reagent II (LAR II), Stop & Glo® (S&G) Reagent. Values presented are means ± S.E. from 3 biological replicates. Root growth was evaluated in ImageJ.

### Effects of synthesized compounds on the elongation of hypocotyl segments and auxin signalling in DR5::LUC *Arabidopsis thaliana* transgenic plants

The elongation experiment was done as described previously (Fendrych et al. 2016; Li et al. 2018). Plates with *Arabidopsis thaliana* seeds expressing DR5::LUC (Moreno-Risueno et al. 2010) in the Col-0 background on sterile ½ MS medium were placed vertically under light for 6 h in a growth chamber at 21 °C. Plates were wrapped with aluminium foil and grown for 3 days vertically at 21 °C.

Petri dishes with 5 mL of depletion media (10 mM KCl, 1 mM MES, adjusted to pH 6 by KOH, 1.5% phytigel, MiliQ water as solvent) were prepared. After solidification, cellophane foil was placed on the surface and damped with liquid depletion medium solution.

Petri dishes with three-day-old seedlings were unwrapped and seedlings with similar hypocotyl length were selected. Decapitation was done by cutting seedlings on the surface of the agar right below the apical hook and above the shoot-root junction to get a hypocotyl segment. For each treatment 6–8 segments were prepared. The segments were transferred onto the cellophane foil on the depletion plate and kept in darkness for 30–60 min to deplete endogenous auxin. Subsequently, hypocotyl segments were transferred onto a treatment plate with the depletion medium supplemented with 0.3% DMSO as a blank control, 0.5 µM IAA as positive control and FL4, FL5 or FL6 at a final concentration of 50 µM with or without 0.5 µM IAA. The treatment plates were placed on a flatbed scanner (Epson, model: V370 Photo) and wet black filter paper was placed inside the lid of the dish to improve the contrast of the image. The samples were scanned in the 8-bit grayscale mode automatically using the AutoIt program and at 1200 dpi every 20 min for 3 h. Afterwards, hypocotyl segments were collected in 2 mL Eppendorf tubes (with 2 iron beads inside) and flash-frozen in liquid nitrogen. Samples were ground with Retsch mill and then 700 µL of Cell Culture Lysis reagent (CCLR, 5× diluted in water) was added. The samples were mixed, centrifuged and left on ice for 2 min. Subsequently, 100 µL of lysate was transferred to a microtiter plate and assayed with a luminometer (BioTek Synergy H1 Plate Reader) using Luciferase Assay Reagent II (LAR II), Stop & Glo®

(S&G) Reagent. Values presented are means ± S.E. from 3 biological replicates. Hypocotyl elongation was evaluated in ImageJ.

### qPCR analysis

Five-day-old seedlings of *Arabidopsis thaliana* wild-type Col-0 were transferred to ½ MS liquid medium supplemented with 0.3% DMSO as a blank control, 1 µM IAA as a positive control or FL5 and FL6 at 20 µM concentration with or without 1 µM IAA. After 3 h seedlings were harvested by flash-freezing in liquid nitrogen. Samples were ground to fine powder in liquid nitrogen using pestle and mortar.

Total RNA was extracted using the Spectrum™ Plant Total RNA Kit, and DNA-free™ Kit was used to remove contaminating DNA. Two µg total RNA was reverse transcribed to cDNA using Oligo(dT)<sub>18</sub> primer and RevertAid H Minus Reverse Transcriptase. Real-time qPCR analysis was performed using a SYBR® Select Master Mix on a Bio-Rad CFX96 Touch Real-Time PCR Detection System. The three-step cycling programme was as follows: 95 °C for 2 min, followed by 40 cycles at 95 °C for 5 s, 60.5 °C for 20 s and 72 °C for 10 s. Melting curve analysis was conducted between 75 and 95 °C. Transcript levels of four auxin-responsive genes, *Lateral organ boundaries-domain 29 - LBD29* (AT3G58190), *Indole-3-acetic acid inducible 5 - IAA5* (AT1G15580), *GRETCHEN HAGEN 3.3 - GH3.3* (AT2G23170), *Auxin response factor 19 - ARF19* (AT1G19220) were quantified, and *beta-tubulin 2 - TUB2* (AT5G62690) was used as an internal reference gene. The primer pairs used for qPCR were: *LBD29* forward 5'-GCCACAGAGAGTAGTTACCAC-3' and reverse 5'-TCACGAGAAGGAGATGTAGCC-3'; *IAA5* forward 5'-CGGCGAAAAAGAGTCAAGTTGTG-3' and reverse 5'-TTTGGTCCGTTCCGAGACTGTTC-3'; *GH3.3* forward 5'-ACAATCCGCTCCACAGTTC-3' and reverse 5'-ACGAGTTCCTTGCTCTCCAA-3'; *ARF19* forward 5'-TGGGAAGAGTTTGTGAACTGC-3' and reverse 5'-TGTACTTTCCAAGCATTCCG-3'; *TUB2* forward 5'-GAGCCTTACAACGCTACTCTGTCTGTC-3' and reverse 5'-ACACCAGACATAGTAGCAGAAATCAAG-3'. The relative transcript abundance was calculated after normalizing with *TUB2*. Expression levels were calculated using the  $\Delta\Delta C_t$  method (Pfaffl 2001). Values presented are means ± S.E. from three biological replicates.

### SPR assay

Surface plasmon resonance (SPR) assay was done in accordance with the previously described protocol (Lee et al. 2014). TIR1 was expressed in insect cell culture

using a recombinant baculovirus. The construct contained sequences for three affinity tags: 10 His, green fluorescent protein (GFP) and FLAG. Protein purified using the His tag was used for SPR assays by passing it over a streptavidin chip loaded with biotinylated IAA7 degron peptide in the absence or presence of IAA and test compounds **FL5** and **FL6** and auxinole as anti-auxin control.

Hepes-buffered saline with 10 mM Hepes, 3 mM EDTA, 150 mM NaCl and 0.05% Tween 20 was used as the SPR buffer. Compounds were premixed with the protein and the binding experiments were run at a flow rate of  $30 \mu\text{L min}^{-1}$  using 2 min of injection time and 4 min of dissociation time. Data from a control channel (a mutated IAA7 peptide) and from a buffer-only run supplemented with DMSO (final 1%) were subtracted from each sensogram following the standard double reference subtraction protocol.

### Uptake quantification in *Arabidopsis thaliana* seedlings using LC-MS/MS

Five-day-old seedlings of *Arabidopsis thaliana* wild-type Col-0 were transferred to plates containing sterile  $\frac{1}{2}$  MS solid media supplemented with 0.3% DMSO as a blank control, or compounds **FL4**, **FL5** and **FL6** at  $10 \mu\text{M}$  concentration. The seedlings were harvested after 1, 3 and 6 h.

To compare the uptake of compound **FL4** and its controls, **CTRL1** and **CTRL2**, five-day-old seedlings were transferred to sterile  $\frac{1}{2}$  MS liquid media supplemented with 0.3% DMSO as a blank control, or compounds **FL4**, **CTRL1** and **CTRL2** at  $10 \mu\text{M}$  concentration. The seedlings were harvested after 30 min.

Immediately after harvest, samples were flash-frozen in liquid nitrogen and divided into five (long feeding) or six (short feeding) biological replicates with  $\approx 10$  mg of plant material each. All the samples were purified by liquid-liquid extraction using combination of acetonitrile/ $\text{H}_2\text{O}$ /hexane (1/1/1) in the  $900 \mu\text{L}$  total volume. Three ceria-stabilized zirconium oxide beads were added, and samples were homogenized by MixerMill MM 301 bead mill (Retsch GmbH, Germany) for 10 min at a frequency 27 Hz. Extracts were then incubated at  $4^\circ\text{C}$  shaking continuously for 15 min and centrifuged (15 min, 23 000 g,  $4^\circ\text{C}$ ). The acetonitrile/ $\text{H}_2\text{O}$  phase was transferred to MicroSpin tubes ( $0.2 \mu\text{m}$ , nylon, Chromservis s.r.o., Czech Republic), centrifuged for 10 min (12 000 g,  $4^\circ\text{C}$ ) and flow-through fraction was evaporated to dryness under vacuum.

The evaporated samples were dissolved in  $50 \mu\text{L}$  of 10% acetonitrile prior to LC-MS/MS analysis using an Acquity UPLC® System (Waters, USA) coupled to a triple quadrupole mass spectrometer Xevo™ TQ MS (Waters MS Technologies, UK). Chromatographic reverse-phase column (Kinetex C18 100 A, length 50 mm, diameter 2.1 mm,

particle size  $1.7 \mu\text{m}$ ; Phenomenex, USA) was used for UHPLC separation. The mobile phase consisted of acetonitrile (A) and deionized water (B), both with the addition of 0.1% acetic acid. Time of each analysis was 5.5 min, flow rate  $0.3 \text{ mL/min}$  and gradient elution as follows: 0 min – 60% B, 3.0 min – 30% B, 4.25 min – 99% B, 4.5 min – 99% B, 5.5 – 60% B. During the analysis, samples were stored in an autosampler at  $4^\circ\text{C}$ ,  $2 \mu\text{L}$  of each sample were injected and column tempered at  $30^\circ\text{C}$ .

The eluate was introduced into the electrospray ion source of a tandem MS analyser in positive mode (ESI+) using these optimized conditions: source/desolvation temperature  $150/600^\circ\text{C}$ ; cone/desolvation gas flow,  $150/1000 \text{ L/h}$ ; capillary voltage, 1 kV; cone voltage, 20 V; collision gas flow,  $0.14 \text{ mL/min}$ . Analytes were measured in multiple reaction monitoring (MRM) mode with optimized conditions as described in Supplementary Table S1 and data interpreted in MassLynx v4.2 software (Waters MS Technologies, UK).

For compound quantification, samples with known compounds concentration were prepared and their recovery factor was calculated. Three replicates of seven-day-old *Arabidopsis thaliana* seedlings were harvested ( $\approx 10$  mg per sample) and flash-frozen in liquid nitrogen. To each sample 1 nmol of **FL4**, **FL5**, **FL6**, **CTRL1** and **CTRL2** was added and samples were processed by LLE as described above. To calculate for analytes losses and matrix effects, six points external calibration curve ranging from 1 fmol to 100 pmol in 10% acetonitrile was measured, and recovery factor was calculated from the samples (Supplementary Table S2). For real samples, concentration was calculated from an external calibration curve after application of dilution and recovery factors.

### Accumulation of the fluorescently labelled derivatives in *Arabidopsis* root cells

Five-day-old seedlings of *Arabidopsis thaliana* wild-type Col-0 or marker lines: p2485-RFP (endoplasmic reticulum marker) (Montesinos et al. 2012), Wave lines 22R/SYP32 (Golgi apparatus marker) (Geldner et al. 2009) were incubated in 24-well plates containing 1 mL of  $\frac{1}{2}$  MS liquid media supplemented with fluorescent compounds **FL4** and **CTRL1** at a final concentration of  $10 \mu\text{M}$  for 10–20 min, while 9R/VAMP711 seedlings (Geldner et al. 2009) were treated with **FL4**, **CTRL1** and **CTRL2** at a final concentration of  $2 \mu\text{M}$  for 3 h. Plants were subsequently visualized using a confocal microscope (ZEISS LSM 800 and LSM 900). Experimental set up involved  $10\times$  –  $100\times$  objective.

## Results and discussion

### Synthesis of the compound library

The planar aromatic ring and a carboxyl group side chain are regarded to be essential for auxin activity; while the amino group of the IAA indole ring is involved in the hydrogen bonding with the amide group of Leu439 in TIR1 receptor (Tan et al. 2007). To ensure selective alkylation of IAA molecule at the  $\alpha$ -position, carboxylic acid and amino groups of commercially available indole-3-acetic acid were protected as methyl esters in accordance with the procedure published by Hayashi et al. (Hayashi et al. 2012). The *tert*-butyl (iodoalkyl)carbamates **2a-d** were prepared from aliphatic amino alcohols *via* Boc-protection of amino group, followed by iodination of hydroxyl group with slight changes to the procedure published by Ensich et al. (Ensich and Hesse 2002). Subsequently,  $\alpha$ -alkylation of IAA dimethyl ester **1** was investigated (Fig. 1). Synthesis was done with slight changes to the procedure published by Chen et al. (Chen et al. 2013). IAA dimethyl ester **1** was treated with sodium hydride and linkers **2a-d** in dimethylformamide at 0 °C and the mixture was stirred at room temperature for 3 h resulting in **3a-d** in 19–48% yield. Fluorescent labelling with 4-chloro-7-nitrobenzofurazan (NBD) or 5-(dimethylamino)naphthalene-1-sulfonyl (DNS, Dansyl) chloride was performed adopting

procedures published by Bielešová et al. (Bielešová et al. 2019) and Saura et al. (Saura et al. 2015). Linker-tagged IAA double methyl ester derivatives **3a-d** were treated with trifluoroacetic acid in dichloromethane at room temperature for 30 min, affording free amines. The latter were treated with triethylamine and NBD- or DNS-chloride in acetonitrile at room temperature for 3 h. This led to the formation of NBD- and DNS-labelled IAA dimethyl esters **4a-d** and **4e-f** in 57–77% and 27–31% overall yield, respectively. The full deprotection of fluorescently labelled IAA dimethyl esters **4a-f** was performed similarly to the procedure published by Bielešová et al. (Bielešová et al. 2019). Compounds **4a-f** were dissolved in methanol, treated with 1 M lithium hydroxide solution and stirred at 50 °C for 4 h. Subsequent acidification with 1 M potassium hydrogen sulfate solution led to the formation of final products **5a-f** in 28–52% yield, which were designated as **FL1-6**. Detailed procedures for the synthesis of the compounds are available in Supplementary Information.

### Determination of biological activity

First of all, the ability of fluorescently labelled auxin derivatives **FL1-6** to affect auxin signalling was evaluated using the *Arabidopsis* transgenic line DR5::GUS (Ulmasov et al. 1997), in which the expression of the  $\beta$ -glucuronidase

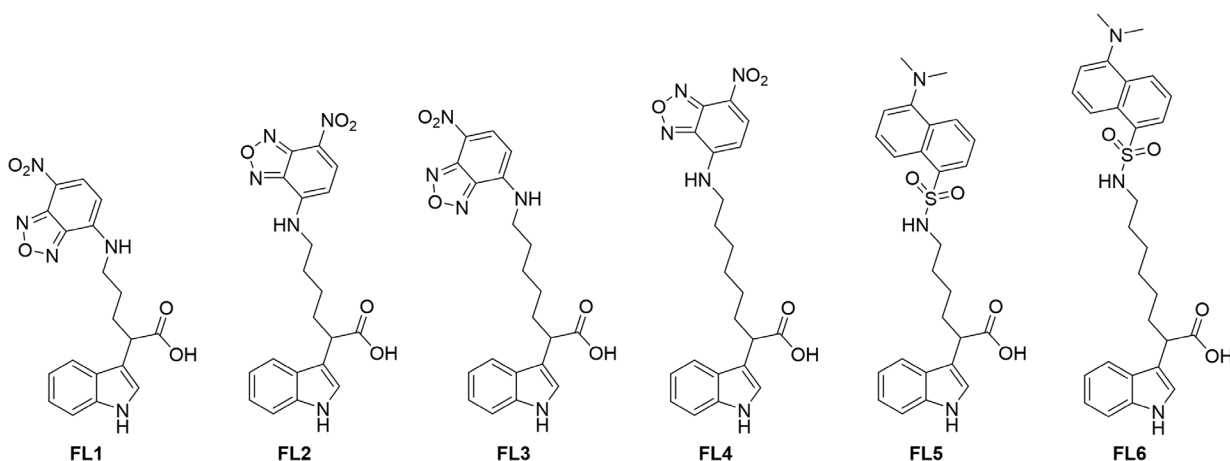
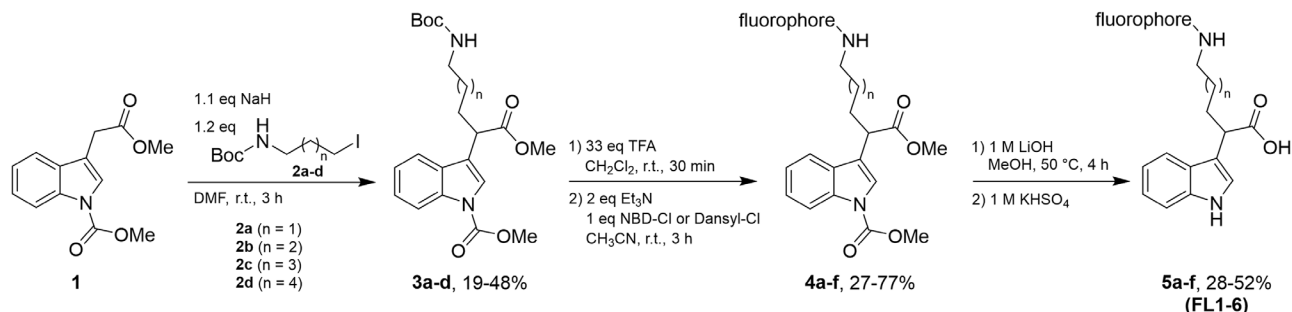
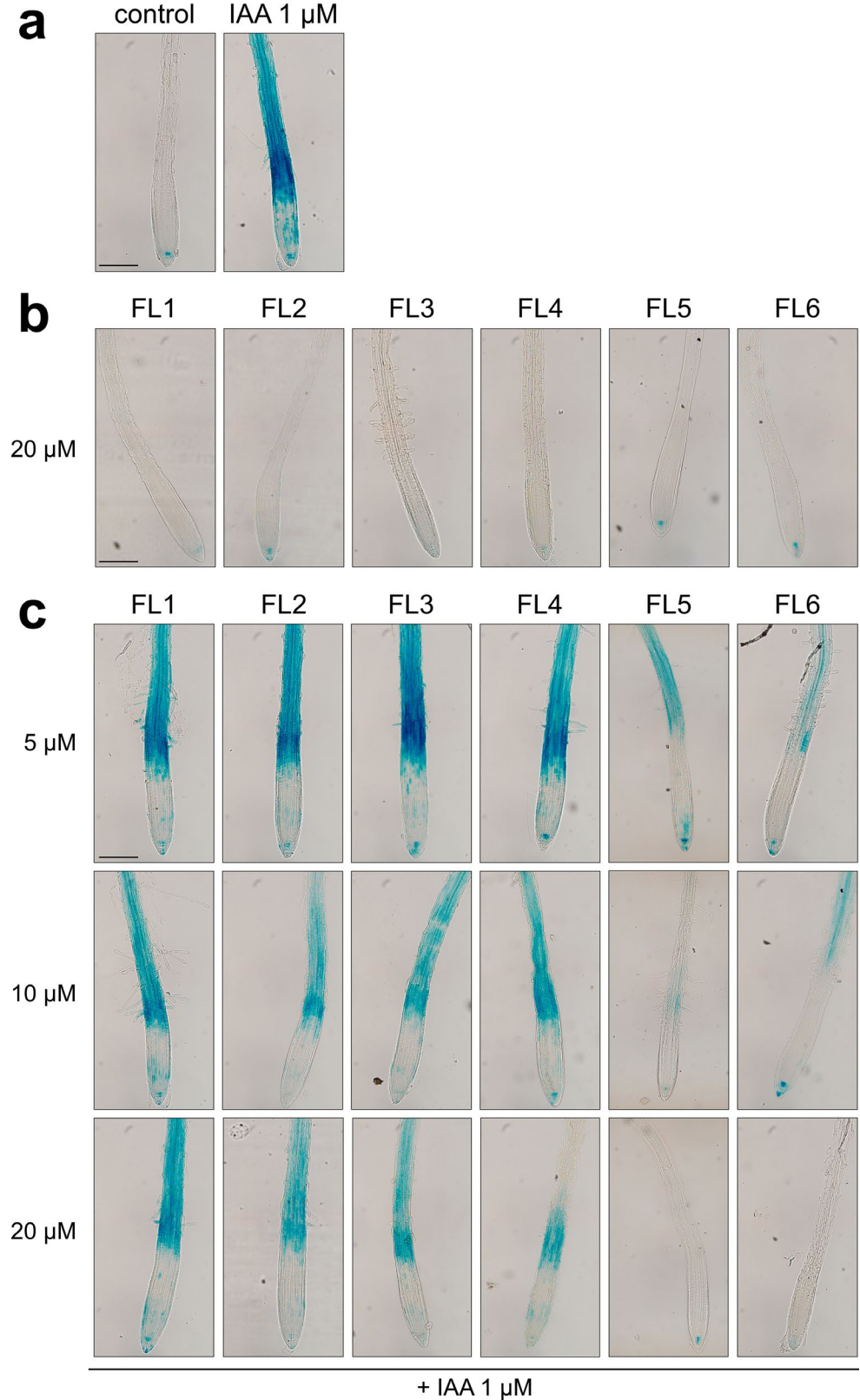


**Fig. 1** Synthesis and structures of fluorescently labelled IAA derivatives **5a-f** designated as **FL1-6**

(GUS) reporter gene is controlled by the synthetic auxin-inducible DR5 promoter. Thus, in contrast to 1  $\mu\text{M}$  IAA treatment, where the roots were stained completely, in

control plants the blue staining was visible only in the root tip, corresponding to the accumulation of endogenous auxins (Fig. 2a). Compounds **FL1-6**, despite being IAA

**Fig. 2** The effect of compounds **FL1-6** on GUS expression in the DR5::GUS transgenic plants of *Arabidopsis thaliana*. Five-day-old seedlings were treated with 1  $\mu\text{M}$  IAA (a), and with compounds 20  $\mu\text{M}$  **FL1-6** for 5 h (b). Five-day-old seedlings were co-treated with compounds **FL1-6** at given concentrations (5, 10 and 20  $\mu\text{M}$ ) and 1  $\mu\text{M}$  IAA for 5 h (c). Figures were chosen as representatives from three independent biological repetitions. Scale bars represents 200  $\mu\text{m}$

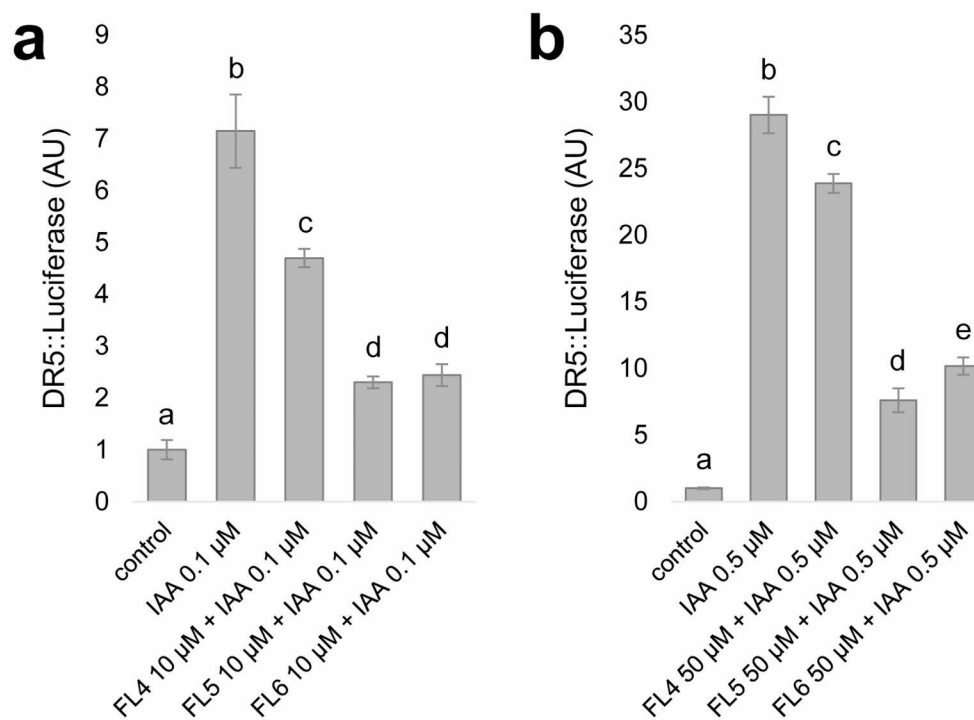


derivatives, did not show auxin activity, manifested by the lack of GUS staining even at 20  $\mu\text{M}$  concentration (Fig. 2b). In contrast, when co-applied with 1  $\mu\text{M}$  IAA (Fig. 2c), some of the fluorescently labelled compounds blocked auxin-induced DR5::GUS expression in a dose-dependent manner, similarly to known anti-auxins (Hayashi et al. 2012). The DNS-labelled compounds **FL5** and **FL6** completely inhibited DR5::GUS expression induced by 1  $\mu\text{M}$  IAA at 20  $\mu\text{M}$  concentration, thus showing the strongest inhibitory effect. Conversely, the longest linker-possessing NBD-labelled compound **FL4** showed weak anti-auxin activity at 20  $\mu\text{M}$  concentration and was not able to completely inhibit effect of 1  $\mu\text{M}$  IAA (Fig. 2c).

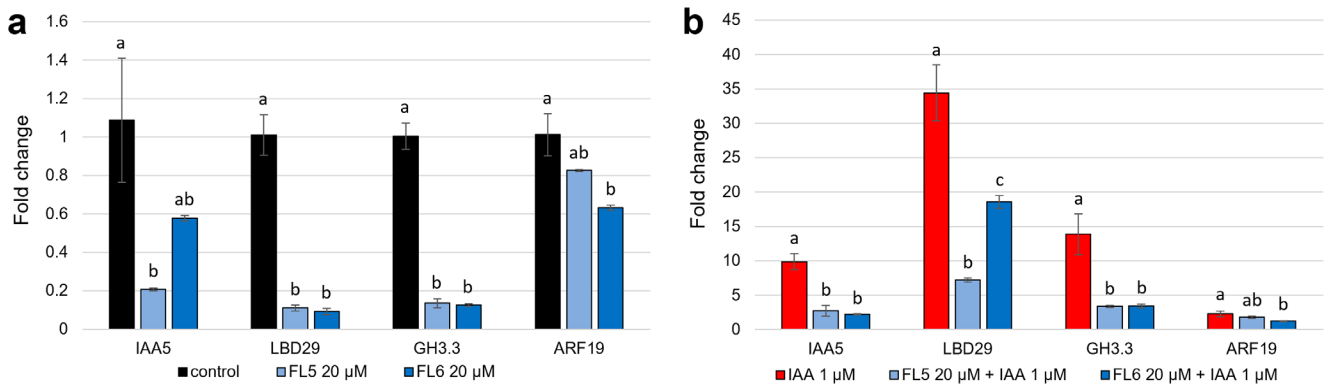
Based on the results from DR5::GUS assay, the most active compounds **FL4**, **FL5** and **FL6** were selected for the investigation of their uptake and stability dynamics *in vivo* by ultra-high performance liquid chromatography coupled with tandem mass spectrometry (UHPLC-MS/MS), to determine the duration over which these compounds can be utilized in *in planta* experiments. Plants were transferred to solid medium treated with 10  $\mu\text{M}$  concentration of **FL4**, **FL5** or **FL6** and subsequently harvested at three time points. After 1 h treatment, all three compounds **FL4**, **FL5** and **FL6** were detected in plants at a similar concentration (Supplementary

Figure S1). Compared to **FL5** and **FL6**, for which the concentration within the first 3 h stayed almost unchanged, the concentration of **FL4** after 3 h was decreased approximately 2-fold, indicating its rapid metabolism or degradation. After 6 h the concentration of all three compounds in plants was drastically reduced (Supplementary Figure S1), indicating that the compounds should be primarily used in short term experiments.

Consequently, **FL4**, **FL5** and **FL6** were further examined for their biological activity in short term assays. For this purpose the transgenic line DR5::LUC (Moreno-Risueno et al. 2010) was employed, which possesses a synthetic auxin-responsive promoter DR5 driving the expression of the firefly luciferase enzyme. In this transgenic line, auxin response is determined by the luminescence intensity of luciferase. Thus, to confirm anti-auxin activity of the compounds, we checked whether treatment with the compounds will lead to a decrease in the nuclear auxin response in IAA co-treated DR5::LUC plants (Moreno-Risueno et al. 2010; Fendrych et al. 2018). Similarly to DR5::GUS results, auxin-induced DR5::LUC response was strongly antagonized by DNS-labelled derivatives **FL5** and **FL6**, showing their inhibitory effect on auxin signalling (Fig. 3a). Moreover, treatment of hypocotyl segments prepared from etiolated DR5::LUC



**Fig. 3** The effect of compounds **FL4**, **FL5** and **FL6** on luciferase activity in roots and hypocotyl segments of DR5::LUC transgenic plants of *Arabidopsis thaliana*. Five-day-old seedlings were transferred to plates with media containing 0.3% DMSO as a blank control, 0.1  $\mu\text{M}$  IAA as positive control or 10  $\mu\text{M}$  **FL4**, **FL5** and **FL6** with 0.1  $\mu\text{M}$  IAA for 6 h. The luminescence intensity in the roots was quantified (a). Hypocotyl segments from three-day-old dark-grown plants were transferred onto a treatment plate with the depletion medium supplemented with 0.3% DMSO as a blank control, 0.5  $\mu\text{M}$  IAA as positive control or compounds **FL4**, **FL5** and **FL6** at final concentration of 50  $\mu\text{M}$  with 0.5  $\mu\text{M}$  IAA for 3 h. The luminescence intensity in the hypocotyls was quantified (b). Results are averages from three independent repetitions. Values are means  $\pm$  S.E. Different letters indicate statistically significant differences between treatments according to Wilcoxon test after Kruskal-Wallis analysis ( $P < 0.05$ )



**Fig. 4** Transcriptional response of auxin-responsive genes to treatment with compounds **FL5** and **FL6**. Five-day-old seedlings were treated with compounds **FL5** and **FL6** at 20  $\mu\text{M}$  alone (**a**) or in co-treatment with 1  $\mu\text{M}$  IAA (**b**) for 3 h. Transcript levels of four early auxin-responsive genes, *LBD29*, *IAA5*, *GH3.3*, *ARF19* were quantified by real-time PCR and fold change was calculated *via* the comparative cycle threshold (Ct) method and values were normalised based on expression of the *TUB2* gene. Values are means  $\pm$  S.E. from three biological repetitions. Different letters indicate statistically significant differences between compounds and control (**a**) or between compounds and IAA (**b**), according to Tukey's test after ANOVA ( $P < 0.05$ )

transgenic plants of *Arabidopsis thaliana* with IAA and DNS-labelled derivatives **FL5** or **FL6** resulted in a significant decrease in luminescence intensity, compared to plants treated with 0.5  $\mu\text{M}$  IAA alone, proving their strong anti-auxin activity also in this tissue (Fig. 3b). The decrease in luminescence intensity in both roots and hypocotyl segments was milder in the case of treatment with **FL4**.

Subsequently, a qPCR analysis of four early auxin-responsive genes, *IAA5*, *LBD29*, *GH3.3* and *ARF19* (Paponov et al. 2008), upon treatment with the most active compounds **FL5** and **FL6** at 20  $\mu\text{M}$  concentration alone or in combination with 1  $\mu\text{M}$  IAA was performed. Compounds **FL5** and **FL6** did not induce the expression of auxin-responsive genes, which further corroborates our initial observation that these compounds do not possess auxin activity (Fig. 4a). In co-treatment with IAA, the compounds suppressed expression of auxin-inducible genes, confirming

their anti-auxin activity (Fig. 4b). Moreover, the compounds were also able to inhibit the effect of endogenous auxin-induced gene expression, which was the most prominent for the *LBD29* and *GH3.3* genes (Fig. 4a).

Additionally, the effect of compounds on primary root-growth and elongation of hypocotyl segments was evaluated (Fig. 5, Supplementary Figure S2). Nanomolar IAA concentrations trigger primary root-growth inhibition (Woodward and Bartel 2005) which has been demonstrated to happen in less than 30 s after auxin reaches the root surface (Fendrych et al. 2018). In rapid root-growth assay, DNS-labelled compounds **FL5** and **FL6** were able to partially reverse the auxin-induced primary root-growth inhibition, confirming their anti-auxin activity (Fig. 5a, Supplementary Figure S2a). In contrast, NBD-labelled derivative **FL4** was unable to counteract the effect of auxin.

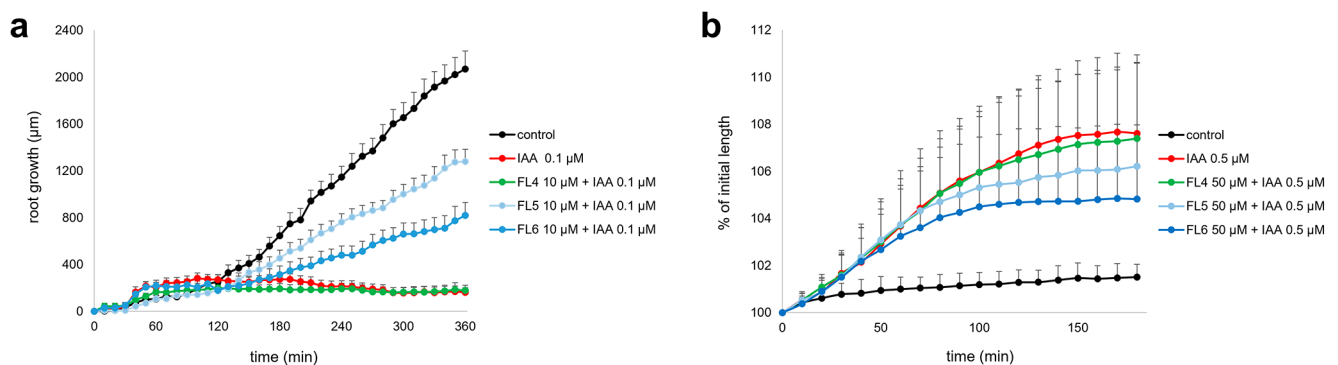


**Fig. 5** The effect of compounds **FL4**, **FL5** and **FL6** on primary root growth and elongation of hypocotyl segments in DR5::LUC transgenic plants of *Arabidopsis thaliana*. Five-day-old seedlings were transferred to plates with media containing 0.3% DMSO as a blank control, 0.1  $\mu\text{M}$  IAA as positive control or 10  $\mu\text{M}$  **FL4**, **FL5** and **FL6** with 0.1  $\mu\text{M}$  IAA for 6 h and primary root growth was evaluated (**a**). Hypocotyl segments from three-day-old dark-grown plants were transferred onto a treatment plate with the depletion medium supplemented with 0.3% DMSO as a blank control, 0.5  $\mu\text{M}$  IAA as positive control or 50  $\mu\text{M}$  **FL4**, **FL5** and **FL6** with 0.5  $\mu\text{M}$  IAA for 3 h and elongation of hypocotyl segments was evaluated (**b**). Results are averages from three independent repetitions. Values are means  $\pm$  S.E.

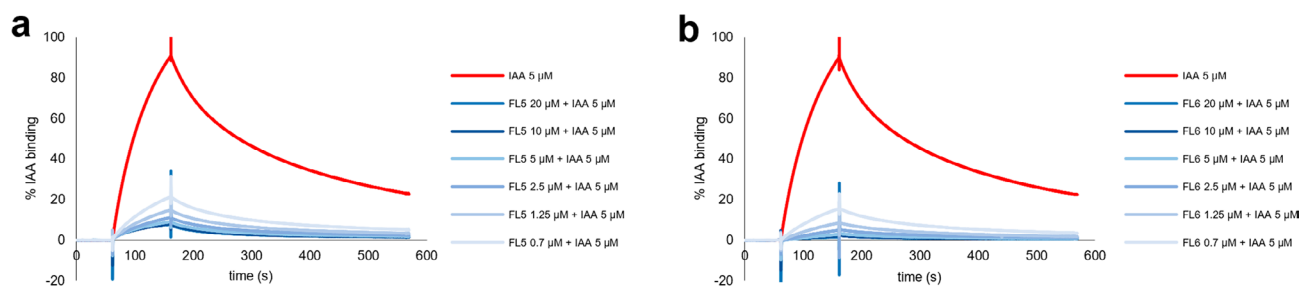


**Fig. 6** SPR analysis of the antagonistic effect of compounds **FL5** and **FL6** on auxin-induced interaction between TIR1 protein and IAA7 degron peptide. The sensorgrams show association followed by dissociation in buffer. Results for IAA (5  $\mu\text{M}$ ) on TIR1 protein alone (red) and in co-treatment with compounds **FL5** (a) and **FL6** (b) in a concentration range (0.7, 1.25, 2.5, 5, 10, 20  $\mu\text{M}$ ) (shades of blue)

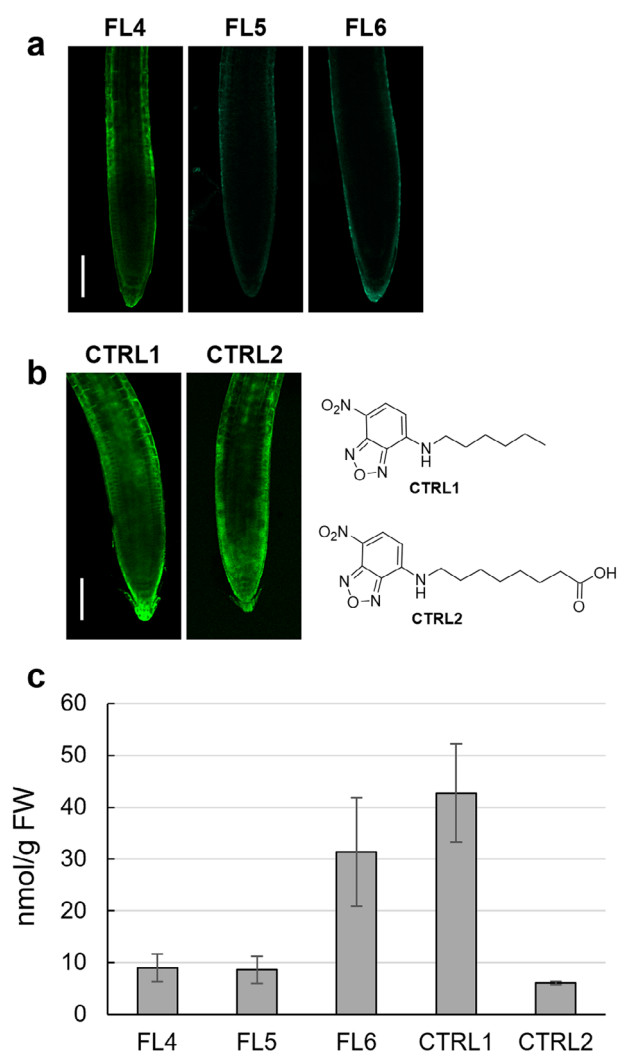


**Fig. 7** Uptake of compounds **FL4-6**, **CTRL1** and **CTRL2** in *Arabidopsis thaliana* roots. Five-day-old seedlings were treated with 10  $\mu\text{M}$  **FL4**, **FL5** and **FL6** for 10 min, 10 $\times$  zoom, scale bar represents 100  $\mu\text{m}$ . (a) Five-day-old seedlings were treated with 10  $\mu\text{M}$  **CTRL1** and **CTRL2** for 10 min, 10 $\times$  zoom, scale bar represents 100  $\mu\text{m}$ ; corresponding structures of controls **CTRL1** and **CTRL2** (b). Uptake of compounds **FL4-6**, **CTRL1** and **CTRL2** was evaluated in five-day-old *Arabidopsis thaliana* seedlings treated with test compounds at 10  $\mu\text{M}$  concentration and harvested after 30 min (c). Results are averages (nmol/g FW) from six biological repetitions. Values are means  $\pm$  S.D.

Nuclear auxin signalling is believed to be involved in elongation of hypocotyl segments (Fendrych et al. 2016). In etiolated hypocotyls of *Arabidopsis thaliana*, which have been depleted of endogenous auxin by decapitation, compounds **FL5** and, particularly, **FL6** were also able to revert IAA-induced hypocotyl elongation, while **FL4** could not (Fig. 5b, Supplementary Figure S2b).

#### In vitro determination of anti-auxin activity by SPR binding assay

The capacity of the derivatives to antagonize auxin binding to auxin receptor TIR1 (Dharmasiri et al. 2005a; Kepinski and Leyser 2005) and AUXIN/INDOLE-3-ACETIC ACID7 (IAA7) co-receptor complex (Calderón Villalobos et al. 2012) was studied by SPR analysis (Lee et al. 2014). Similarly, to other anti-auxins (Hayashi et al. 2012; Žukauskaitė et al. 2023), derivatization of the IAA molecule at the  $\alpha$ -position resulted in anti-auxin activity of the compounds. In co-treatment with 5  $\mu\text{M}$  IAA, compounds inhibited TIR1 co-receptor assembly with IAA7 degron (Fig. 6) by competing with IAA for its binding site and reducing the signal in a dose dependent manner. Interestingly, DNS-labelled derivatives **FL5** (Fig. 6a) and **FL6** (Fig. 6b) showed stronger anti-auxin activity, outperforming auxinole (Hayashi et al. 2012) (Supplementary Figure S3).

#### Fluorescence properties and validation of compound uptake in planta

To evaluate the suitability of the compounds for microscopy experiments, their fundamental fluorescence properties were evaluated in vitro. As anticipated, in methanol, compound **FL4** had absorption maxima at 467 nm, and emission maxima at 531 nm, resulting in 64 nm Stokes shift typical for NBD-labelled molecules (Lancet and Pecht 1977; Bielešová et al. 2019). On the other hand, compounds **FL5** and **FL6** had absorption maxima between 331 and 336 nm, and emission maxima at 519–520 nm, resulting in large

Stokes shifts, typical for DNS derivatives (Wei et al. 2023) (Supplementary Figure S4, Supplementary Table S3).

The uptake of compounds **FL4**, **FL5** and **FL6** in *Arabidopsis thaliana* after treatment in liquid medium was evaluated using confocal microscopy and UHPLC-MS/MS (Fig. 7a,c). Due to its superior fluorescence properties, compound **FL4** was the most suitable for confocal experiments. Distribution of **FL4** in *Arabidopsis thaliana* roots was mainly observed in epidermal cells. DNS-labelled compounds **FL5** and **FL6**, which possessed absorption maxima in UV range, could not be properly visualized using the excitation lasers available in our equipment (minimum wavelength of 405 nm), and therefore only low-clarity images could be obtained (Fig. 7a). UHPLC-MS/MS results confirmed the accumulation of compounds **FL4**, **FL5** and **FL6** in plants, indicating that the poor visibility of **FL5** and **FL6** in confocal images is not uptake-related (Fig. 7c). However, compounds **FL5** and **FL6** could probably be used in UV-microscopy experiments, which typically employ microscopes equipped with excitation lasers within the UV spectrum (Maxfield and Wüstner 2012).

Based on the fluorescence measurements in vitro and visualization of compounds in primary roots of *Arabidopsis thaliana*, compound **FL4** was selected to study accumulation patterns *in planta*, alongside of two selected controls **CTRL1** and **CTRL2** (synthesis in Supplementary Information), which are possible degradation products of compound **FL4** (Fig. 7b). The uptake of these control compounds **CTRL1** and **CTRL2** in *Arabidopsis thaliana* after treatment in liquid medium was analogously evaluated using

confocal microscopy and UHPLC-MS/MS. From the results, we could see that **CTRL1** accumulated strongly in *Arabidopsis* roots (Fig. 7b,c), which may be caused by its lipophilic nature (Schriever and Lamshoeft 2020). **CTRL2** also showed a uniform accumulation in all root layers, although the uptake was lower than that of **CTRL1** (Fig. 7b,c).

### Visualization of subcellular distribution of compound **FL4** and its controls

Compound **FL4** and its controls **CTRL1** and **CTRL2** were used to investigate their accumulation patterns at the subcellular level. Both, compound **FL4** and **CTRL1**, displayed strong co-localization with the fluorescent signal of the transgenic marker lines p24δ5-RFP and SYP32-mCherry, revealing their accumulation in endoplasmic reticulum and Golgi apparatus (Fig. 8). The localization of **CTRL1** to both organelles suggests that the auxin part of **FL4** might not be crucial for compound accumulation in endoplasmic reticulum and Golgi apparatus.

To study accumulation in vacuoles, two controls, **CTRL1** and carboxylic acid group bearing **CTRL2**, were used alongside compound **FL4** (Fig. 9). In the case of **FL4**, a co-localization with tonoplast using VAMP711-mCherry marker line could be seen after 3 h (Fig. 9a). Moreover, a partial co-localization with the marker is also visible for carboxylic acid group bearing **CTRL2** (Fig. 9c). On the contrary, **CTRL1** did not show co-localization with the marker (Fig. 9b).

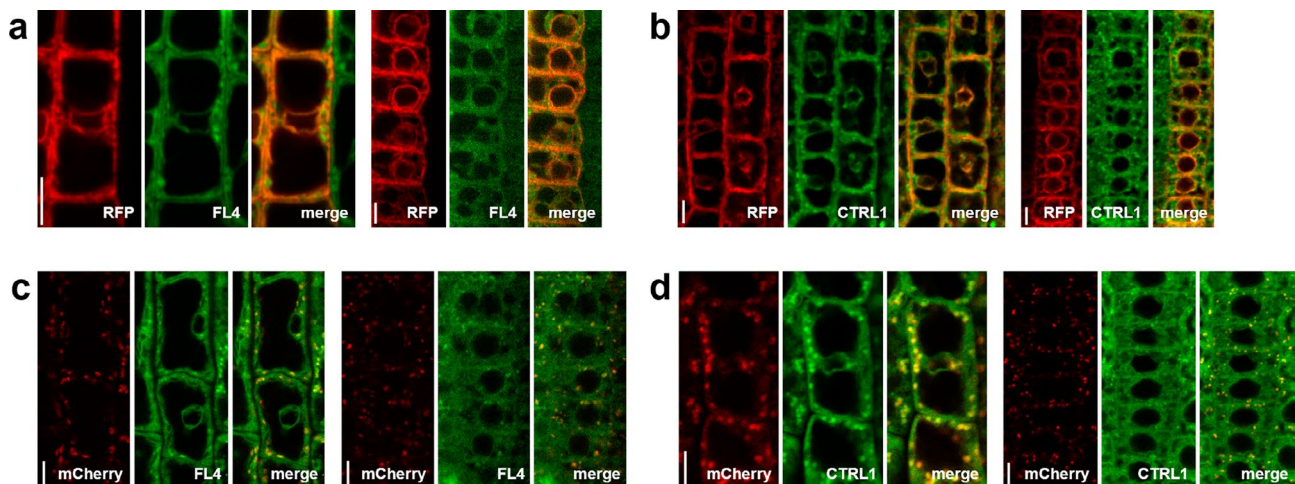


**Fig. 8** Uptake of **FL4** and **CTRL1** in epidermal cells of the root meristematic zone of *Arabidopsis thaliana* roots of p24δ5-RFP (a,b), and SYP32-mCherry (c,d) lines. Five-day-old seedlings were treated with 10 μM **FL4** (a,c) and **CTRL1** (b,d) for 10–20 min. 40× zoom for **CTRL1** or 100× zoom for **FL4**. Scale bars represent 5 μm

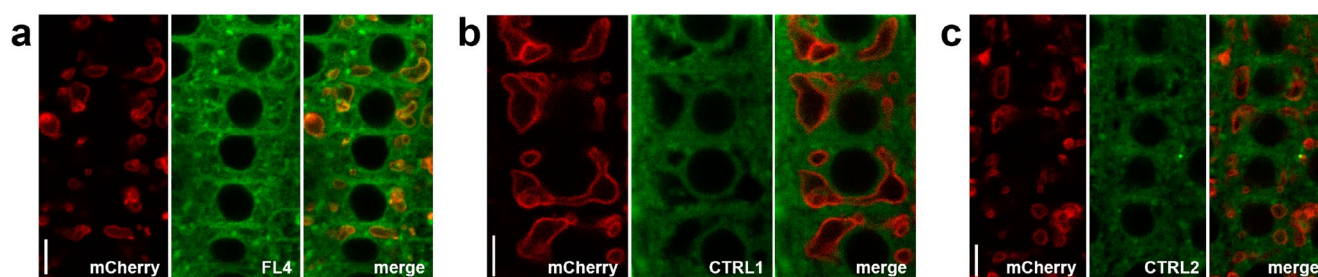


**Fig. 9** Uptake of **FL4**, **CTRL1** and **CTRL2** in epidermal cells of the root meristematic zone of *Arabidopsis thaliana* roots of VAMP711-mCherry line. Five-day-old seedlings were treated with **FL4** (a), **CTRL1** (b), and **CTRL2** (c) at 2  $\mu$ M concentration for 3 h. 40 $\times$  or 100 $\times$  zoom. Scale bars represent 5  $\mu$ m

## Conclusions

In this work we have designed and synthesized six new fluorescently labelled IAA derivatives. None of the compounds showcased auxin activity but, on the contrary, acted as anti-auxins at levels of developmental regulation, transcription induction, and binding to receptors.

While NBD-labelled compounds **FL1-4** only possessed weak anti-auxin activity, DNS-labelled compounds **FL5** and **FL6** were able to completely inhibit auxin-induced expression of DR5::GUS transcriptional auxin response reporter. Further testing using another auxin-responsive reporter line, DR5::LUC, revealed stronger anti-auxin activity of **FL5** and **FL6** compounds in roots and hypocotyls in comparison with compound **FL4**. qPCR analysis, performed with the most active compounds **FL5** and **FL6** alone and in co-treatment with IAA, showed decreased expression of early auxin response genes. Anti-auxin activity of compounds was also confirmed by SPR binding assays, where **FL5** and **FL6** showed strong anti-auxin activity, outperforming the established anti-auxin auxinole (Hayashi et al. 2012).

Fluorescence measurements showed that the DNS derivatives are not suitable for most confocal experiments, due to their absorption maxima being around 331–336 nm, which is in the UV part of the spectrum. The compound **FL4**, bearing NBD as a fluorescent label, showed better fluorescent properties and was used for further studies of accumulation patterns *in planta*. Two additional compounds (**CTRL1** and **CTRL2**), which also carried the NBD label in the structures but lacked the auxin molecule, were also prepared to be used as controls. The results from visualization of subcellular localization show that **CTRL1**, despite not having an auxin molecule attached, was able to mimic the accumulation patterns of **FL4**, even at the subcellular level. In the case of the vacuolar marker VAMP711-mCherry, co-localization was visible for compound **FL4** and **CTRL2**, both of which carry a carboxylic acid group in the structure. Due to the relatively strong co-localizations of the **FL4** compound

and controls **CTRL1** and **CTRL2**, **FL4** is not suitable for studying auxin accumulation patterns *in planta*. Notably, the strongest anti-auxin activity possessing compounds **FL5** and **FL6** might be used to study mechanism of binding to auxin receptors and for *in planta* manipulations of auxin-regulated processes with potential applications in agriculture.

**Supplementary Information** The online version contains supplementary material available at <https://doi.org/10.1007/s10725-023-01083-0>.

**Acknowledgements** The authors would like to thank Karolína Kubišová and Iñigo Saiz-Fernández for valuable scientific discussions.

**Authors' contributions** Conceptualization – AŽ. Methodology – KB, PH, MK, RN, FB, ZG, LF, IK, ON, JF, AŽ. Investigation – KB, PH, MK, RN, AŽ. Formal analysis – KB, PH, MK, RN, FB, JF, AŽ. Visualization – KB, PH, AŽ. Data Curation – KB, MK, RN, ON, AŽ. Resources – AŽ, RN, MS, KD, ON, JF. Writing - Original Draft – KB. Writing - Review & Editing – AŽ, JF. All authors have read and agreed to the published version of the manuscript.

**Funding** Open access publishing supported by the National Technical Library in Prague. This work was supported by the Palacký University Olomouc Young Researcher Grant Competition (JG\_2020\_002), by the Internal Grant Agency of Palacký University Olomouc (IGA\_PrF\_2023\_016, IGA\_PrF\_2023\_031), by the Ministry of Education, Youth and Sports of the Czech Republic through the European Regional Development Fund-Project Plants as a tool for sustainable global development (CZ.02.1.01/0.0/0.0/16\_019/0000827) and the project Support of mobility at Palacký University Olomouc II. (CZ.02.2.69/0.0/0.0/18\_053/0016919). The Biacore T200 SPR instrument was provided by the WISB Research Technology Facility within the School of Life Sciences, University of Warwick.

Open access publishing supported by the National Technical Library in Prague.

**Data Availability** The data that supports the findings of this study are available from the corresponding authors upon reasonable request.

## Declarations

**Competing interests** On behalf of all authors, the corresponding author states that there is no conflict of interest.

**Open Access** This article is licensed under a Creative Commons Attribution 4.0 International License, which permits use, sharing, adaptation, distribution and reproduction in any medium or format, as long as you give appropriate credit to the original author(s) and the source, provide a link to the Creative Commons licence, and indicate if changes were made. The images or other third party material in this article are included in the article's Creative Commons licence, unless indicated otherwise in a credit line to the material. If material is not included in the article's Creative Commons licence and your intended use is not permitted by statutory regulation or exceeds the permitted use, you will need to obtain permission directly from the copyright holder. To view a copy of this licence, visit <http://creativecommons.org/licenses/by/4.0/>.

## References

- Balcerowicz M, Shetty KN, Jones AM (2021) Fluorescent biosensors illuminating plant hormone research. *Plant Physiol* 187:590–602. <https://doi.org/10.1093/plphys/kiab278>
- Bielešová K, Pařízková B, Kubeš M et al (2019) New fluorescently labeled auxins exhibit promising anti-auxin activity. *N Biotechnol* 48:44–52. <https://doi.org/10.1016/j.nbt.2018.06.003>
- Brannon JH, Magde D (1978) Absolute quantum yield determination by thermal blooming. *Fluorescein*. *J Phys Chem* 82:705–709. <https://doi.org/10.1021/j100495a018>
- Calderón Villalobos LIA, Lee S, De Oliveira C et al (2012) A combinatorial TIR1/AFB-Aux/IAA co-receptor system for differential sensing of auxin. *Nat Chem Biol* 8:477–485. <https://doi.org/10.1038/nchembio.926>
- Caumon H, Vernoux T (2023) A matter of time: Auxin signaling dynamics and the regulation of auxin responses during plant development. *J Exp Bot* 132. <https://doi.org/10.1093/jxb/erad132>
- Chen J, Kassenbrock A, Li BX, Xiao X (2013) Discovery of a potent anti-tumor agent through regioselective mono-N-acylation of 7H-pyrrolo[3,2-f]quinazoline-1,3-diamine. *Medchemcomm* 4:1275–1282. <https://doi.org/10.1039/c3md00134b>
- Dharmasiri N, Dharmasiri S, Estelle M (2005a) The F-box protein TIR1 is an auxin receptor. *Nature* 435:441–445. <https://doi.org/10.1038/nature03543>
- Dharmasiri N, Dharmasiri S, Weijers D et al (2005b) Plant development is regulated by a family of auxin receptor F box proteins. *Dev Cell* 9:109–119. <https://doi.org/10.1016/j.devcel.2005.05.014>
- Dindas J, Scherzer S, Roelfsema MRG et al (2018) AUX1-mediated root hair auxin influx governs SCF<sup>TIR1/AFB</sup>-type Ca<sup>2+</sup> signaling. *Nat Commun* 9. <https://doi.org/10.1038/s41467-018-03582-5>
- Ensch C, Hesse M (2002) Total syntheses of the spermine alkaloids (-)-(R,R)-hopromine and (±)-homaline. *Helv Chim Acta* 85:1659–1677. [https://doi.org/10.1002/1522-2675\(200206\)85:6<1659::AID-HLCA1659>3.0.CO;2-D](https://doi.org/10.1002/1522-2675(200206)85:6<1659::AID-HLCA1659>3.0.CO;2-D)
- Fendrych M, Leung J, Friml J (2016) TIR1/AFB-Aux/IAA auxin perception mediates rapid cell wall acidification and growth of *Arabidopsis* hypocotyls. *Elife* 5. <https://doi.org/10.7554/eLife.19048.001>
- Fendrych M, Akhmanova M, Merrin J et al (2018) Rapid and reversible root growth inhibition by TIR1 auxin signalling. *Nat Plants* 4:453–459. <https://doi.org/10.1038/s41477-018-0190-1>
- Friml J (2022) Fourteen stations of auxin. *Cold Spring Harb Perspect Biol* 14:a039859. <https://doi.org/10.1101/cshperspect.a039859>
- Friml J, Gallei M, Gelová Z et al (2022) ABP1–TMK auxin perception for global phosphorylation and auxin canalization. *Nature* 609:575–581. <https://doi.org/10.1038/s41586-022-05187-x>
- Geisler M (2018) Seeing is better than believing: visualization of membrane transport in plants. *Curr Opin Plant Biol* 46:104–112. <https://doi.org/10.1016/j.pbi.2018.09.005>
- Geldner N, Dénervaud-Tendon V, Hyman DL et al (2009) Rapid, combinatorial analysis of membrane compartments in intact plants with a multicolor marker set. *Plant J* 59:169–178. <https://doi.org/10.1111/j.1365-313X.2009.03851.x>
- Grossmann K (2010) Auxin herbicides: current status of mechanism and mode of action. *Pest Manag Sci* 66:113–120. <https://doi.org/10.1002/ps.1860>
- Guilfoyle TJ, Hagen G (2007) Auxin response factors. *Curr Opin Plant Biol* 10:453–460. <https://doi.org/10.1016/j.pbi.2007.08.014>
- Hasegawa J, Sakamoto T, Fujimoto S et al (2018) Auxin decreases chromatin accessibility through the TIR1/AFBs auxin signaling pathway in proliferative cells. *Sci Rep* 8. <https://doi.org/10.1038/s41598-018-25963-y>
- Hayashi KI, Neve J, Hirose M et al (2012) Rational design of an auxin antagonist of the SCF<sup>TIR1</sup> auxin receptor complex. *ACS Chem Biol* 7:590–598. <https://doi.org/10.1021/cb200404c>
- Hemelíková N, Žukauskaitė A, Pospíšil T et al (2021) Caged phytohormones: from chemical inactivation to controlled physiological response. *J Agric Food Chem* 69:12111–12125. <https://doi.org/10.1021/acs.jafc.1c02018>
- Herud-Sikimić O, Stiel AC, Kolb M et al (2021) A biosensor for the direct visualization of auxin. *Nature* 592:768–772. <https://doi.org/10.1038/s41586-021-03425-2>
- Jiang K, Asami T (2018) Chemical regulators of plant hormones and their applications in basic research and agriculture. *Biosci Biotechnol Biochem* 82:1265–1300. <https://doi.org/10.1080/09168451.2018.1462693>
- Kepinski S, Leyser O (2005) The *Arabidopsis* F-box protein TIR1 is an auxin receptor. *Nature* 435:446–451. <https://doi.org/10.1038/nature03542>
- Kimura T, Haga K, Shimizu-Mitao Y et al (2018) Asymmetric auxin distribution is not required to establish root phototropism in *Arabidopsis*. *Plant Cell Physiol* 59:823–835. <https://doi.org/10.1093/pcp/pcy018>
- Lace B, Prandi C (2016) Shaping small bioactive molecules to untangle their biological function: a focus on fluorescent plant hormones. *Mol Plant* 9:1099–1118. <https://doi.org/10.1016/j.molp.2016.06.011>
- Lancet D, Pecht I (1977) Spectroscopic and immunochemical studies with nitrobenzoxadiazolealanine, a fluorescent dinitrophenyl analog. *16:5150–5157*. <https://doi.org/10.1021/bi00642a031>
- Lee S, Sundaram S, Armitage L et al (2014) Defining binding efficiency and specificity of auxins for SCF<sup>TIR1/AFB</sup>-Aux/IAA co-receptor complex formation. *ACS Chem Biol* 9:673–682. <https://doi.org/10.1021/cb400618m>
- Li L, Krens SFG, Fendrych M, Friml J (2018) Real-time analysis of auxin response, cell wall pH and elongation in *Arabidopsis thaliana* hypocotyls. *Bio Protoc* 8. <https://doi.org/10.21769/bioprotoc.2685>
- Liang Y, Jiang C, Liu Y et al (2020) Auxin regulates sucrose transport to repress petal abscission in rose (*Rosa hybrida*). *Plant Cell* 32:3485–3499. <https://doi.org/10.1105/TPC.19.00695>
- Ma L, Li G, Li S, Jiang S (2020) An improved protocol for whole mount clearing of plant root tip. *Chin Bull Bot* 55:596–604. <https://doi.org/10.11983/CBB20016>
- Malachowska-Ugarte M, Sperduto C, Ermolovich YV et al (2015) Brassinosteroid-BODIPY conjugates: design, synthesis, and properties. *Steroids* 102:53–59. <https://doi.org/10.1016/j.steroids.2015.07.002>
- Maxfield FR, Wüstner D (2012) Analysis of cholesterol trafficking with fluorescent probes. *Methods Cell Biol* 108:367–393. <https://doi.org/10.1016/B978-0-12-386487-1.00017-1>

- Mockaitis K, Estelle M (2008) Auxin receptors and plant development: a new signaling paradigm. *Annu Rev Cell Dev Biol* 24:55–80. <https://doi.org/10.1146/annurev.cellbio.23.090506.123214>
- Montesinos JC, Sturm S, Langhans M et al (2012) Coupled transport of Arabidopsis p24 proteins at the ER–Golgi interface. *J Exp Bot* 63:4243–4261. <https://doi.org/10.1093/jxb/ers112>
- Moreno-Risueno MA, Van Norman JM, Moreno A et al (2010) Oscillating gene expression determines competence for periodic Arabidopsis root branching. *Science* (1979) 329:1306–1311. <https://doi.org/10.1126/science.1191937>
- Okushima Y, Overvoorde PJ, Arima K et al (2005) Functional genomic analysis of the AUXIN RESPONSE FACTOR gene family members in Arabidopsis thaliana: Unique and overlapping functions of ARF7 and ARF19. *Plant Cell* 17:444–463. <https://doi.org/10.1105/tpc.104.028316>
- Overvoorde PJ, Okushima Y, Alonso JM et al (2005) Functional genomic analysis of the AUXIN/INDOLE-3-ACETIC ACID gene family members in Arabidopsis thaliana. *Plant Cell* 17:3282–3300. <https://doi.org/10.1105/tpc.105.036723>
- Paponov IA, Paponov M, Teale W et al (2008) Comprehensive transcriptome analysis of auxin responses in *Arabidopsis*. *Mol Plant* 1:321–337. <https://doi.org/10.1093/mp/ssm021>
- Pařízková B, Pernisová M, Novák O (2017) What has been seen cannot be unseen—detecting auxin in vivo. *Int J Mol Sci* 18:2736. <https://doi.org/10.3390/ijms18122736>
- Pfaffl MW (2001) A new mathematical model for relative quantification in real-time RT-PCR. *Nucleic Acids Res* 29:e45. <https://doi.org/10.1093/nar/29.9.e45>
- Prandi C, Ghigo G, Occhiato EG et al (2014) Tailoring fluorescent strigolactones for in vivo investigations: a computational and experimental study. *Org Biomol Chem* 12:2960–2968. <https://doi.org/10.1039/c3ob42592d>
- Qi L, Kwiatkowski M, Chen H et al (2022) Adenylate cyclase activity of TIR1/AFB auxin receptors in plants. *Nature* 611:133–138. <https://doi.org/10.1038/s41586-022-05369-7>
- Remington DL, Vision TJ, Guilfoyle TJ, Reed JW (2004) Contrasting modes of diversification in the Aux/IAA and ARF gene families. *Plant Physiol* 135:1738–1752. <https://doi.org/10.1104/pp.104.039669>
- Rigal A, Ma Q, Robert S (2014) Unraveling plant hormone signaling through the use of small molecules. *Front Plant Sci* 5. <https://doi.org/10.3389/fpls.2014.00373>
- Santner A, Calderon-Villalobos LIA, Estelle M (2009) Plant hormones are versatile chemical regulators of plant growth. *Nat Chem Biol* 5:301–307. <https://doi.org/10.1038/nchembio.165>
- Sauer M, Robert S, Kleine-Vehn J (2013) Auxin: simply complicated. *J Exp Bot* 64:2565–2577. <https://doi.org/10.1093/jxb/ert139>
- Saura AV, Marín MJ, Burguete MI et al (2015) The synthesis of new fluorescent bichromophoric compounds as ratiometric pH probes for intracellular measurements. *Org Biomol Chem* 13:7736–7749. <https://doi.org/10.1039/c5ob00704f>
- Scheuring D, Löffke C, Krüger F et al (2016) Actin-dependent vacuolar occupancy of the cell determines auxin-induced growth repression. *Proc Natl Acad Sci U S A* 113:452–457. <https://doi.org/10.1073/pnas.1517445113>
- Schriever C, Lamshoef M (2020) Lipophilicity matters – a new look at experimental plant uptake data from literature. *Sci Total Environ* 713. <https://doi.org/10.1016/j.scitotenv.2020.136667>
- Šenkyřík JB, Krivánková T, Kaczorová D, Štefelová N (2023) Investigation of the effect of the auxin antagonist PEO-IAA on cannabinoid gene expression and content in *Cannabis sativa* L. plants under in vitro conditions. *Plants* 12:1664. <https://doi.org/10.3390/plants12081664>
- Shani E, Weinstain R, Zhang Y et al (2013) Gibberellins accumulate in the elongating endodermal cells of Arabidopsis root. *Proc Natl Acad Sci U S A* 110:4834–4839. <https://doi.org/10.1073/pnas.1300436110>
- Smýkalová I, Vrbová M, Cvečková M et al (2019) The effects of novel synthetic cytokinin derivatives and endogenous cytokinins on the in vitro growth responses of hemp (*Cannabis sativa* L.) explants. *Plant Cell Tissue Organ Cult* 139:381–394. <https://doi.org/10.1007/s11240-019-01693-5>
- Suzuki K, Kobayashi A, Kaneko S et al (2009) Reevaluation of absolute luminescence quantum yields of standard solutions using a spectrometer with an integrating sphere and a back-thinned CCD detector. *Phys Chem Chem Phys* 11:9850–9860. <https://doi.org/10.1039/b912178a>
- Tamaki H, Reguera M, Abdel-Tawab YM et al (2015) Targeting hormone-related pathways to improve grain yield in rice: a chemical approach. *PLoS ONE* 10. <https://doi.org/10.1371/journal.pone.0131213>
- Tan X, Calderon-Villalobos LIA, Sharon M et al (2007) Mechanism of auxin perception by the TIR1 ubiquitin ligase. *Nature* 446:640–645. <https://doi.org/10.1038/nature05731>
- Todd OE, Figueiredo MRA, Morran S et al (2020) Synthetic auxin herbicides: finding the lock and key to weed resistance. *Plant Sci* 300. <https://doi.org/10.1016/j.plantsci.2020.110631>
- Ulmasov T, Hagen G, Guilfoyle TJ (1997) ARF1, a transcription factor that binds to auxin response elements. *Science* 276:1865–1868. <https://doi.org/10.1126/science.276.5320.1865>
- Wei P, Xiao L, Gou Y et al (2023) A novel peptide-based relay fluorescent probe with a large Stokes shift for detection of Hg<sup>2+</sup> and S<sup>2-</sup> in 100% aqueous medium and living cells: visual detection via test strips and smartphone. *Spectrochim Acta A Mol Biomol Spectrosc* 285. <https://doi.org/10.1016/j.saa.2022.121836>
- Woodward AW, Bartel B (2005) Auxin: Regulation, action, and interaction. *Ann Bot* 95:707–735. <https://doi.org/10.1093/aob/mci083>
- Žukauskaitė A, Saiz-Fernández I, Bielešová K et al (2023) New PEO-IAA-inspired anti-auxins: synthesis, biological activity, and possible application in hemp (*Cannabis sativa* L.) micropropagation. <https://doi.org/10.1007/s00344-023-11031-x>. *J Plant Growth Regul*

**Publisher's Note** Springer Nature remains neutral with regard to jurisdictional claims in published maps and institutional affiliations.